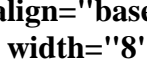


Biophysical Journal, Volume 99

Supporting Material

Title: Pores formed by Bax **5 relax to a smaller size and keep at equilibrium**

Gustavo Fuertes, Ana J. García-Sáez, Santi Esteban-Martín,
Diana Giménez, Orlando L. Sánchez-Muñoz, Petra Schwille, and Jesus Salgado

Supplementary Material for

Pores formed by Bax α 5 relax to a smaller size and keep at equilibrium

Gustavo Fuertes,[†] Ana J. García-Sáez,^{‡§} Santi Esteban-Martín,^{†¶} Diana Giménez,[†] Orlando L. Sánchez-Muñoz,[†] Petra Schwille,[‡] Jesús Salgado^{†*}

[†]*Instituto de Ciencia Molecular, Universidad de Valencia, Catedrático José Beltrán 2, 46980 Paterna (Valencia), Spain;* [‡]*Biotechnologisches Zentrum der TU Dresden, Tatzberg 47/49, 01307 Dresden, Germany.*

[§]*Present address: Max Planck Institute for Metals Research and German Cancer Research Center, Bioquant, Im Neuenheimer Feld 267, 69120 Heidelberg, Germany.* [¶]*Present address: Institute for Research in Biomedicine, Parc Científic, Baldiri Reixac 10, 08028 Barcelona, Spain.*

This file contains one Table and five Figures.

Table S1. Numbers of total analyzed GUVs and those completely porated, partially porated or non porated, for different P/L values and successive dye entrances. We also include the percentage values of porated GUVs (completely refilled plus partially refilled), over the total number of analyzed GUVs, and of GUVs with stable pores, over the total number of porated GUVs.

P/L	Dye	Total analyzed	Completely refilled ^a	Partially refilled ^b	Non porated	Porated (% from total)	With stable pores (% from all porated) ^c
0	1	101	5	3	93	8	-
	2	101	5	0	98	5	63
1/720	1	371	70	20	281	24	-
	2	371	70	0	301	19	78
	3	371	70	0	301	19	78
1/90	1	152	74	2	76	50	-
	2	152	74	0	76	49	97
	3	152	74	0	76	49	97
1/22.5	1	94	85	0	9	90	-
	2	94	85	0	9	90	100
	3	94	85	0	9	90	100

^a Corresponding to *all-or-none* leakage

^b Corresponding to the *graded* leakage

^c GUVs with stable pores are defined as those which exhibit leakage for the first dye and also for successive dyes. They are found to be all (and exclusively) of the all-or-none type.

Figures

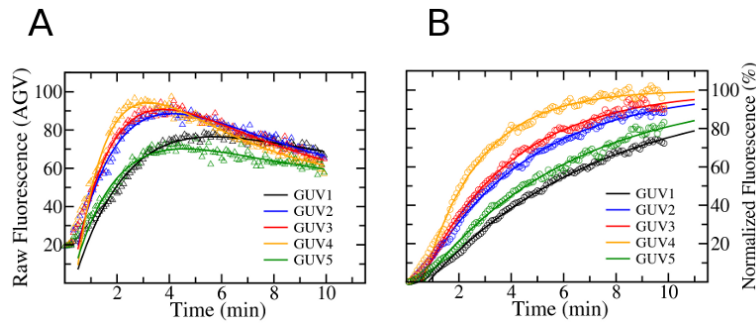


Fig. S1 Examples illustrating the quantitative analysis and normalization of long-term kinetics from the influx of the second dye. The same method was used for the analysis of kinetics of the third dye. For the second and third leakage events, the dyes were added to the external solution after GUVs were for long time incubating in presence of the peptide (120 and 135 min, respectively) and the fluorescence was immediately registered. Thus, dye entrance occurs in parallel to the dilution of the dye from the point of addition. The change with time of the outside fluorescence $F_t^{out'}$, which can be measured in some chosen outside points (not shown), follows a first order exponential decay of the type $F_t^{out'} = F_\infty^{out} + F_0^{out} e^{-kt}$, where F_0^{out} and F_∞^{out} are, respectively, fitted values of the outside fluorescence at time 0 and at equilibrium, and k is the decay constant of the outside fluorescence. However, we find that this dilution decay is variable depending on the point where it is measured. Because of this complex time dependence of the outside fluorescence, the kinetics of dye entrance cannot be easily normalized as is done in the case of the entrance of the first dye (which was well equilibrated in the outside solution before and during the measurements). Instead, the raw fluorescence data from the inside of GUVs F_t (measured in average gray values, AGV), shown in A, were fit with the exponential function $F_t = F_0 + (F_t^{out'} - F_0) \times (1 - e^{-3J_v t/R})$ (1) relating it to $F_t^{out'}$, the vesicle radius R (in μm , measured in the images of GUVs) and the volume flux J_v (in $\mu\text{m}/\text{min}$), where F_0 is the initial raw inside-fluorescence. The kinetic traces of each GUV can then be normalized for better comparison between successive leakage events using the equation $F_t^N = (F_t - F_0) / (F_t^{out'} - F_0)$ (shown in B). The normalized kinetics are also represented in Fig. 3E of the main text.

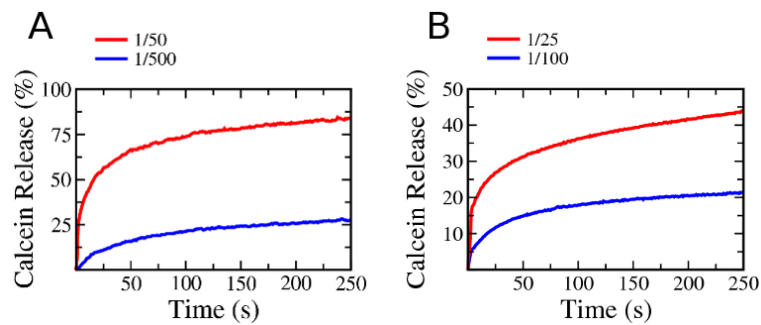


Fig. S2 Short term pore activities measured as kinetics of release of encapsulated calcein in suspensions of LUVs. Examples for two lipid compositions are shown: A) Calcein leakage from POPC LUVs. B) Calcein leakage from POPC:CL (80:20) LUVs. In both cases the kinetics were recorded immediately after addition of Bax α 5 under gentle continuous agitation at the bulk P/L values indicated by the legends. The pore activity is expressed as a percentage of calcein release. The levels at 250 s were used for the bar graphs shown in Fig. 2 of the main text.

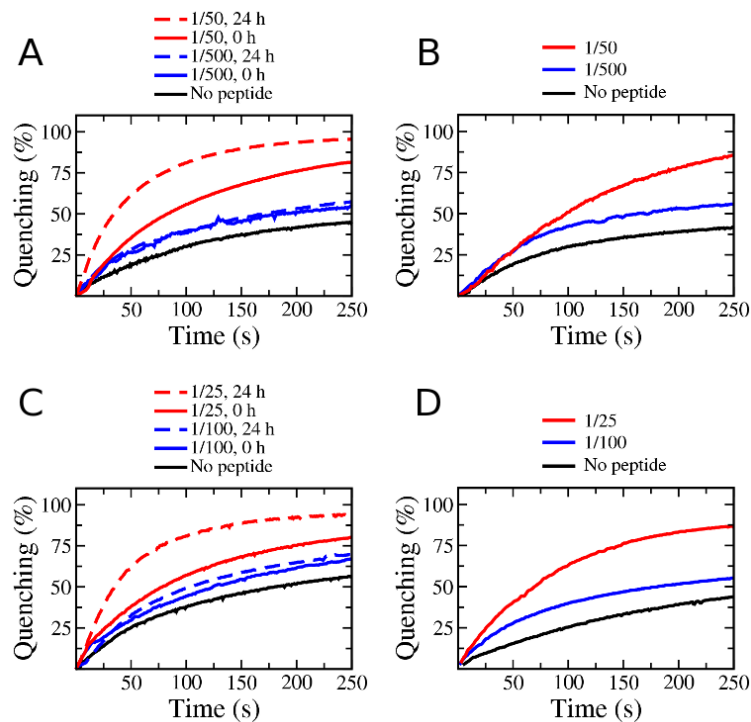


Figure S3. Kinetics of reduction of NBD-PE lipids by dithionite, measured at different times after addition of Bax α 5 and in reconstituted systems. A and C) are NBD-PE quenching kinetics in suspensions of symmetrically labeled POPC:NBD-PE (99.5:0.5) LUVs and POPC:CL:NBD-PE (79.5:20:0.5) LUVs, respectively, in the absence of Bax α 5 (control, black line) or in the presence of this peptide added at bulk P/L ratios indicated in the legends. The kinetics were recorded immediately after peptide addition (solid lines) or after 24 hours incubation with the peptide (dashed lines). B and D) NBD-PE quenching kinetics for POPC:NBD-PE (99.5:0.5) LUVs and POPC:CL:NBD-PE (79.5:20:0.5) LUVs, respectively, prepared in the presence of Bax α 5 at bulk P/L ratios indicated in the legends. The black line is a control with no added peptide registered in the same series of experiments. Because the reduction of the fluorescence lipids by dithionite is much slower than the leakage activity, the kinetics correspond to such a quenching reaction. However, 250 s after addition of dithionite the reaction can be considered substantially completed and quenching levels at that time are essentially proportional to the amount of fluorescent lipids accessible to dithionite. We have used such levels to compute differences with respect to levels with no added peptide (expanded to 100% scale, see Methods in the main text), which were then plotted in Fig. 2.

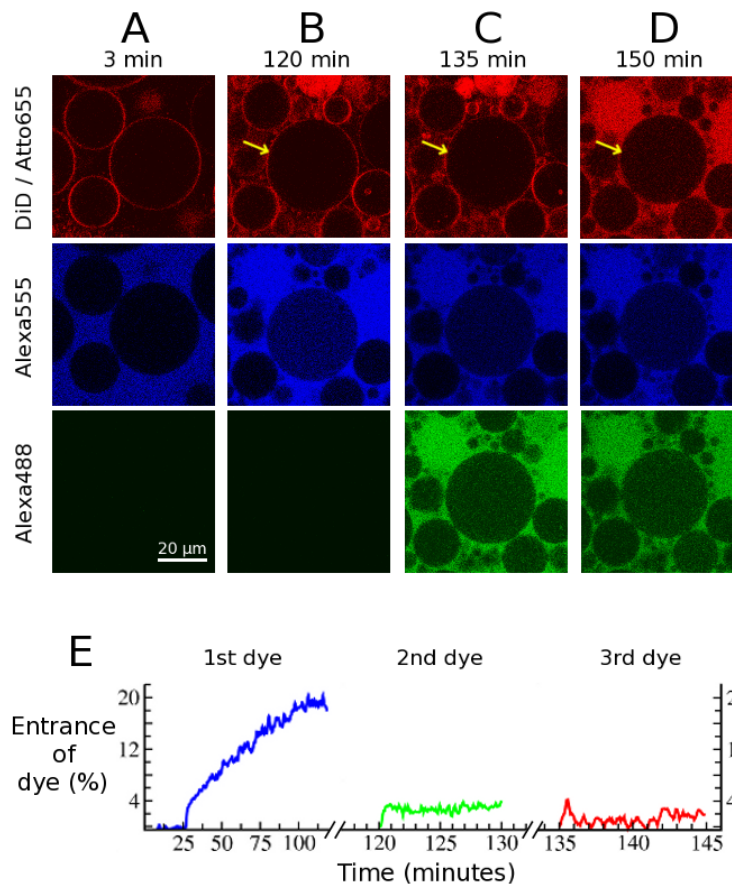


Figure S4. Successive leak-in kinetics of serially added dyes at short and long times showing partial refilling of GUVs and eventually pore closure. Bax α 5 and a first dye (Alexa555, blue) are initially present in the observation chamber, where GUVs labeled with DiD (red) are added to P/L=1/90 (time=0). A) After 3 min the GUVs have sink and fluorescence images start being recorded in three channels. The entrance of the first dye is still delayed for some minutes, and eventually GUVs become permeabilized stochastically (each at a different time). Most of the GUVs are rapidly refilled with dye (see Table S1 and Figure 3 in the main text), but some exhibit a graded refilling (slow and eventually stopped). An example kinetics of graded refilling is shown in the bottom graph. B) Pictures taken two hours latter show that GUVs kept their integrity (red), but some (22% of porated ones at P/L = 1/720, like the one marked with an arrow) have refilled partially with the first dye (compare red and blue channels). Immediately after, a second dye (Alexa488, green) is added. The same GUV as before is now not permeable to the second dye (bottom graph). C). Immediately after, a third dye (Atto655, red) is added, but the same GUV as before keeps impermeable (bottom graph). D) Images taken \sim 15 min after third dye addition.

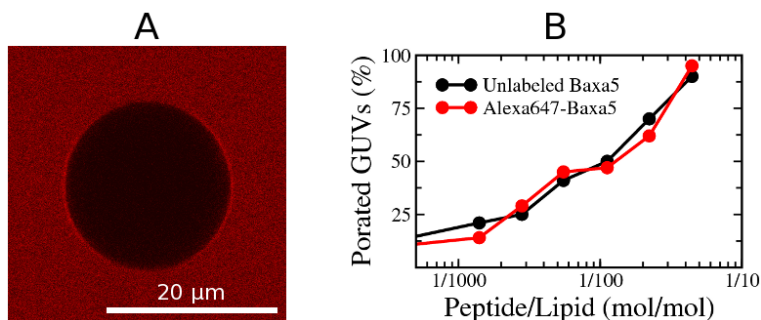


Figure S5. Controls for experiments with GUVs reconstituted in the Alexa647-labeled Bax α 5. A) Unlabeled POPC:CL (80:20) GUVs bathed in a solution containing Alexa647 at a 1 μ M concentration. Although the probe exhibits some binding to the lipid membrane, this is by far smaller than the accumulation in the membrane observed for Alexa647-Bax α 5. B) Dose/response plot for unlabeled Bax α 5 and for Alexa647-Bax α 5. For each P/L value, the points represented are percentages of all porated GUVs counted after two hours in contact with Bax α 5 (black) or Alexa647-Bax α 5 (red), relative to a total of 100 individual GUVs.

References

- Schön P., A. J. García-Sáez, P. Malovrh, K. Bacia, G. Anderluh, and P. Schwille. 2008. Equinatoxin II permeabilizing activity depends on the presence of sphingomyelin and lipid phase coexistence. *Biophys. J.* 95:691-8.